Orbiton-mediated multiphonon scattering in $La_{1-x}Sr_xMnO_3$

K.-Y. Choi,[1,2] P. Lemmens,[3,4] G. Güntherodt,[2] Yu. G. Pashkevich,[5] V. P. Gnezdilov,[6] P. Reutler,[7,8] L. Pinsard-Gaudart,[8] B. Büchner,[7] and A. Revcolevschi[8]

[1]*Institute for Materials Research, Tohoku University, Katahira 2-1-1, Sendai 980-8577, Japan*
[2]*II. Physikalisches Institut, RWTH Aachen, 52056 Aachen, Germany*
[3]*Max Planck Institute for Solid State Research, D-70569 Stuttgart, Germany*
[4]*Institute for Physics of Condensed Matter, TU Braunschweig, D-38106 Braunschweig, Germany*
[5]*A. A. Galkin Donetsk Phystech NASU, 83114 Donetsk, Ukraine*
[6]*B. I. Verkin Institute for Low Temperature Physics NASU, 61164 Kharkov, Ukraine*
[7]*Institute for Solid State Research, IFW Dresden, D-01171 Dresden, Germany*
[8]*Laboratoire de Physico-Chimie, Université Paris-Sud, 91405 Orsay, France*

(Received 14 December 2004; published 14 July 2005)

We report on Raman scattering measurements of single crystalline $La_{1-x}Sr_xMnO_3$ ($x=0$, 0.06, 0.09, and 0.125), focusing on the high-frequency regime. We observe multiphonon scattering processes up to fourth order which show distinct features: (i) anomalies in peak energy and its relative intensity and (ii) a pronounced temperature, polarization, and doping dependence. These features suggest a mixed orbiton-phonon nature of the observed multiphonon Raman spectra.

DOI: 10.1103/PhysRevB.72.024301 PACS number(s): 78.30.−j, 61.72.Hh, 71.27.+a, 71.38.−k

I. INTRODUCTION

Recently, there has been a debate about the underlying nature of the experimentally reported orbitons observed by Raman spectroscopy in orbital ordered $LaMnO_3$.[1] Despite pronounced temperature- and symmetry-dependent properties of the modes, the assignment has been confronted with criticism and alternative concepts.[2–5] For instance, multiphonon scattering has been theoretically predicted to arise from the Franck-Condon (FC) process via self-trapped orbitons.[5] Interestingly, in spite of *mutually exclusive* selection rules, an infrared absorption study shows similar features as Raman scattering measurements at about 125 meV (1000 cm^{-1}), 145 meV (1160 cm^{-1}), and 160 meV (1280 cm^{-1}).[2] This was attributed to multiphonon scattering instead of orbital excitations. On the other hand, orbiton-phonon mixed modes are predicted to appear as satellite structures in the phonon spectrum due to electron-phonon coupling.[4]

$LaMnO_3$ shows $d_{3x^2-r^2}/d_{3y^2-r^2}$ orbital ordering below $T_{JT}=780$ K accompanied by a cooperative Jahn-Teller (JT) distortion.[6] Two different contributions to this antiferro-orbital ordering, which support each other, have been suggested. The first mechanism relies on the cooperative JT effect. In this case, orbiton excitations accompany lattice distortions and vice versa. Their energy, determined by the strength of electron-phonon coupling, is between 0.7 and 2 eV.[5] The second mechanism is based on superexchange interaction. Within this mechanism, orbitons are collective excitations and their energy is expected at much lower energies of 160 MeV because of strong on-site Coulomb repulsion.[7,8] Thus, the determination of the respective contribution to orbital ordering and its energy scale are closely related to the nature of orbital excitations.

Quite recently, resonant Raman scattering measurements[9] have shown a symmetry-dependent resonance of the one- and two-phonon signals around the JT gap at 2 eV, suggesting a phononic origin of the assigned orbitons due to the FC mechanism. However, detailed temperature and symmetry dependence are still lacking, which is significant in addressing a coupling of multiphonon modes to the orbital ordering pattern. Thus, a careful examination on the higher-energy regime of the Raman spectrum above 1300 cm^{-1} is indispensable to uncover all aspects of orbital dynamics. Furthermore, their doping dependence can give further clues because the orbital ordering undergoes a transition while crossing the phase boundary between the canted antiferromagnetic insulating (CAF) and ferromagnetic insulating (FMI) states.[10]

In this paper we report on Raman scattering measurements of single crystalline $La_{1-x}Sr_xMnO_3$ ($x=0$, 0.06, 0.09, and 0.125), focusing on the higher-energy regime. For $x=0$ we observe multiphonon scattering up to fourth order of the one-phonon modes at frequencies between 490 and 640 cm^{-1}. The distinct symmetry temperature and doping dependencies of this scattering contribution unveil the insufficiency of the FC mechanism in describing the observed multiphonon scattering. This points to an orbiton-phonon mixed nature of the observed multiphonon scattering.

II. EXPERIMENTAL DETAILS

Single crystals of $La_{1-x}Sr_xMnO_3$ ($x=0$, 0.06, 0.09, and 0.125) were grown by using the floating zone method. These samples are twinned. As a result, some crystallographic axes cannot be discriminated. Raman scattering measurements were performed in a quasibackscattering geometry with the excitation line $\lambda=514.5$ nm (2.34 eV) of an Ar^+ laser. The small incident power of 8 mW avoids significant heating and irradiation effects. Raman spectra were collected by a DILOR-XY triple spectrometer and a nitrogen cooled CCD detector. The high-temperature measurements from 300 to 640 K were carried out using a heating stage under vacuum.

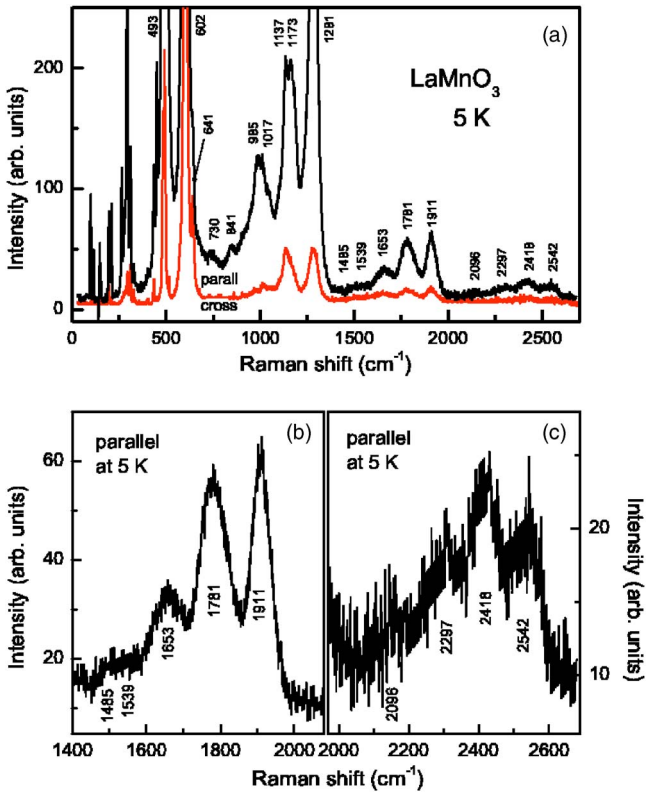

FIG. 1. (Color online) (a) Polarized Raman spectra of $LaMnO_3$ at 5 K in parallel (upper curve) and crossed (lower curve) polarizations. Remarkably, multiphonon scatterings are observed up to fourth order. (b) and (c) A zoom on the modes that correspond to scattering of third and fourth order, respectively.

III. EXPERIMENTAL RESULTS

Figure 1(a) displays polarized Raman spectra of $LaMnO_3$ at 5 K. The incident and scattered light rays are parallel and perpendicular to the quasicubic surface of the perovskite-like crystals. For such scattering geometries, Raman spectra are expected in the xx, $x'x'$, xy, and $x'y'$ polarizations, where x, y, x', and y' correspond to the respective quasicubic [100], [010], [110], and [1$\bar{1}$0] directions. Since the studied samples are twinned, the parallel configuration contains xx and $x'x'$ polarizations, while the crossed one consists of xy and $x'y'$ polarizations. Due to different selection rules, the Raman spectra of the parallel and crossed polarizations show a slightly different behavior in the total number of phonon modes and their relative intensities.

Below 650 cm^{-1} we observe 17 phonon modes as first-order scattering out of 24 symmetry-allowed modes for the *Pnma* crystal structure. The number and sharpness of the observed modes guarantees a high quality of the single crystal. The modes below 330 cm^{-1} are due to vibrations of (La/Sr) cations and rotations of the MnO_6 octahedra. The modes above 400 cm^{-1} arise from bending and stretching vibrations of the octahedra.[11] The atomic displacement of the respective normal modes has been provided by Iliev *et al.*[12] For the detailed physics of the one-phonon modes we refer to our previous work.[13] Hereafter, we will focus on the high-frequency regime covering the reported orbitons. Our results reproduce well the three features at about 1000, 1160, and 1280 cm^{-1} that were assigned to orbitons.[1] Moreover, at much higher energies, additional maxima show up. All maxima between 1485 and 1911 cm^{-1} as well as between 2096 and 2542 cm^{-1} appear close to periodically [see Figs. 1(b) and 1(c)]. This suggests a common origin based on the one-phonon modes between 493 and 641 cm^{-1}. Thus, the claimed orbitons should not be considered as *pure* orbital waves. In principle, a collective orbital wave might be also observable besides multiphonon scattering. However, we did not find evidence for this collective state below 3000 cm^{-1} ($\approx$360 meV). If present, this might be due to a negligible scattering cross section caused by the strong JT distortion. This implies that the orbital ordering in $LaMnO_3$ is predominantly determined by the JT mechanism. A closer look at the higher-energy maxima reveals a fine structure. This is due to a twinning of the single crystal and the polarization dependence of the multiphonon frequency. The latter feature is unusual in conventional multiphonon scattering and allows us to assign the symmetry of the maxima by comparison to the Raman study of an untwinned single crystal.[1]

TABLE I. Peak frequencies of multiphonon scattering of different orders. Multiples of first-order scattering frequencies are given in parentheses. The multiphonon scattering peaks are grouped according to their overtones of the 493, 602, and 641 cm^{-1} modes. Two different frequencies which belong to the same group are attributed to different polarizations.

First	Polarization	Second	Third	Fourth
493	(xx)	985 (986)	1485 (1488)	(1972)
	($x'x'$)	1017	1539	2096
602	(xx)	1137	1653	2297
	($x'x'$)	1173 (1204)	1781 (1806)	2418 (2408)
641	(xx,$x'x'$)	1281 (1282)	1911 (1923)	2542 (2564)

The measured frequencies of the high-energy excitations are listed in Table I together with calculated integer multiples of one-phonon modes. Here, note that the assignment of two-phonon peaks to specific one-phonon modes is not straightforward since two-phonon scattering arises predominantly from regions of the Brillouin zone where the phonon density of states is largest. Nonetheless, as a starting point we will assign them to simple multiples of one-phonon peaks. This is because the FC mechanism is asserted to be mainly responsible for the observed multiphonon scattering.[9,14] In this local mechanism, higher-order scattering usually shows up at integer multiples of one-phonon peak energy, as the FC process results from a displacement of the intermediate electronic state from the initial one rather than a simultaneous emission of n phonons. Thus, this feature enables us to check the validity of the FC mechanism.

The 985 and 1485 cm^{-1} peaks correspond to the overtones of the 493 cm^{-1} mode in xx polarization. The 1017, 1539, and 2096 cm^{-1} peaks might also be related to higher-order scattering of the 493 cm^{-1} mode in $x'x'$ polarization. Similarly, the 1137 (1173), 1653 (1781), and 2297 (2418) cm^{-1} modes are assigned to the overtones of the 602 cm^{-1} mode in xx ($x'x'$) polarization. The 1281, 1911, and 2542 cm^{-1}

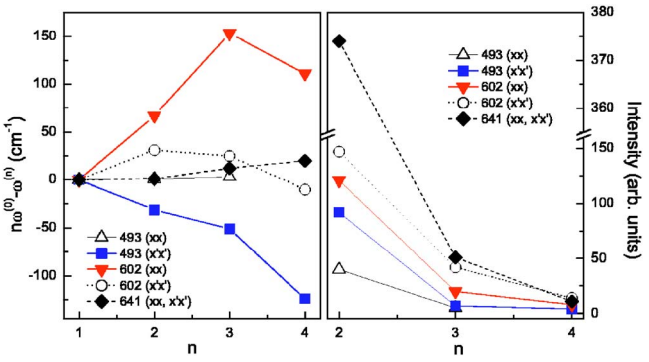

FIG. 2. (Color online) (a) The individual energy differences between n-phonon scattering and integer multiples of one-phonon peaks as a function of order. The energy difference is not equal to zero. In particular, the overtones of the 493 cm^{-1} ($x'x'$) and 602 cm^{-1} (xx) modes show a linear behavior up to third order. A deviation from such a feature is seen at fourth order. (b) The integrated intensity of higher-order phonon spectra. Especially, the 641 cm^{-1} mode shows a strong decrease of scattering intensity with increasing order.

modes correspond to the overtones of the 641 cm^{-1} mode. Several distinct features show up. The second-order scattering at 1281 cm^{-1} is much more intense than the first-order one at 641 cm^{-1}. Furthermore, as Fig. 2(a) displays, there are energy differences between multiphonon scattering and integer multiples of one-phonon peaks. For example, the overtones of the 602 cm^{-1} mode in xx polarization shift to higher energy up to third order and then show a decrease at fourth order. In contrast, those of the 493 cm^{-1} mode in $x'x'$ polarization shift to lower energy with increasing order. The overtones of the 641 cm^{-1} mode show no substantial anomaly in frequency. Instead, its scattering intensity as a function of order does not parallel other modes, contrary to the FC picture. As a consequence of a strong decrease of scattering intensity at fourth order, it becomes weaker than that of the 602 cm^{-1} mode in $x'x'$ polarization [see Figs. 1(c) and 2(b)]. This demonstrates that the FC mechanism cannot capture the full aspect of the observed multiphonon scattering. Further note that even if one considers a combination of first-order peaks, one cannot produce consistently all higher-order peaks.[15]

We turn now to the temperature dependence of the higher-order Raman spectra. As Fig. 3 shows, upon heating, the second-order maxima undergo a broadening and softening. The third- and fourth-order signals (not shown here) can be detected up to 350 and 150 K, respectively. Their behavior parallels that of the second-order signal within the measured temperature interval. The main features are summarized in Fig. 4. First, with increasing temperature, the normalized intensity of the one-phonon mode as well as of their overtones falls off like an order parameter [see Fig. 4(a) for a typical behavior at 493 cm^{-1}]. Second, the second-order mode softens by 40 cm^{-1} upon heating from 5 to 640 K. The representative example at 1281 cm^{-1} is shown in Fig. 4(a). This is contrasted by a small frequency shift of the corresponding one-phonon mode by $\sim$6 cm^{-1}. Noticeably, its temperature dependence agrees well with that of the phonon intensity.

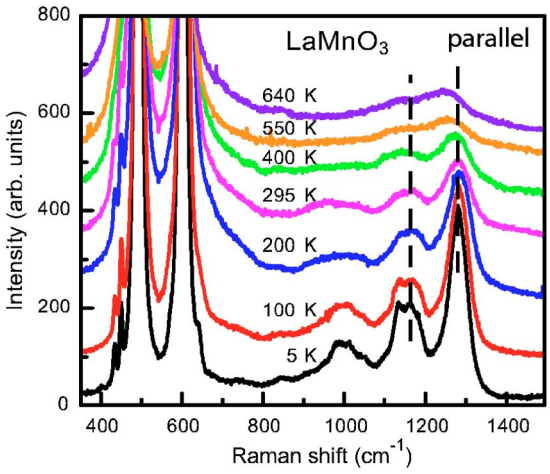

FIG. 3. (Color online) Polarized Raman spectra of $LaMnO_3$ as a function of temperature. The spectra are shifted for clarity.

Third, the ratio of a second- to first-order integrated phonon intensity, I_2/I_1, decreases gradually with increasing temperature, as Fig. 4(b) shows.

Figure 5 displays a doping study of the second-order Raman spectra of $La_{1-x}Sr_xMnO_3$ (x=0, 0.06, 0.09, and 0.125) at 5 K. For the CAF samples (x=0, 0.06, and 0.09) similar features are observed with increasing doping, except for a rapid decrease of the intensity. In contrast, there exists only a broadened maximum around 1000 cm^{-1} in the FMI sample (x=0.125), while maxima around 1160 and 1280 cm^{-1} disappear. It should be noted that the peak energies and relative intensities of the corresponding one-phonon modes do not change appreciably.[13] Furthermore, for x=0.125 the broadened peak around 1000 cm^{-1} should not be considered as the reappearance of the peak that is already present in the CAF samples. Rather, it should be ascribed to a damping of the maxima of the CAF samples ranging from

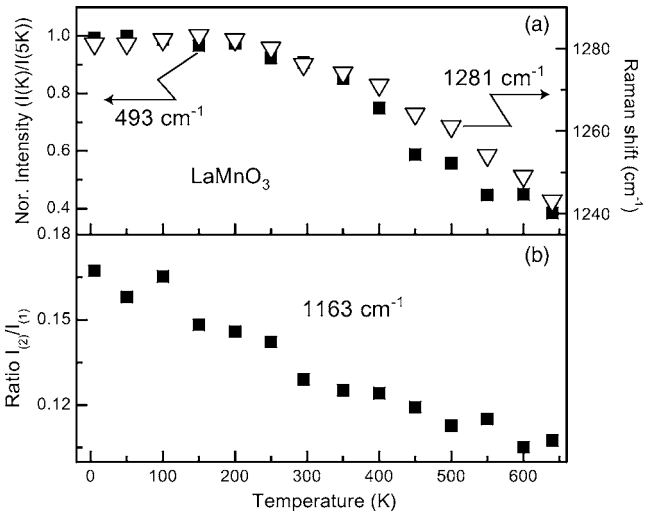

FIG. 4. (a) Temperature dependence of the normalized intensity of the 493-cm^{-1} mode as well as the peak energy of the 1281 cm^{-1} mode. (b) The ratio of second- to first-order scattering at 1163 cm^{-1} as a function of temperature.

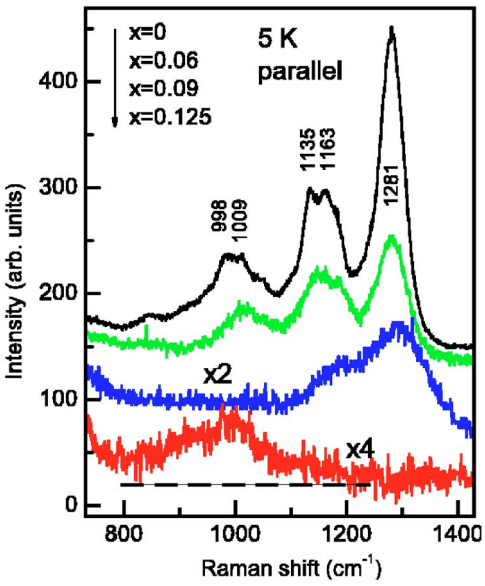

FIG. 5. (Color online) Second-order Raman spectra of $La_{1-x}Sr_xMnO_3$ at 5 K as a function of doping (x=0, 0.06, 0.09, and 0.125).

1100 to 1350 cm^{-1}. This is supported by the results of oxygen-doped manganites $LaMnO_{3+\delta}$ ($0.071 \leqslant \delta \leqslant 0.125$); the three pronounced peaks in the CAF sample continuously evolve into a broad, unstructured maximum in the FMI samples, which systematically shifts to lower energy as δ increases.[16]

In Fig. 6(a) we provide a polarization dependence of the x=0.06 sample due to the discrimination between in-plane and the z axis. Remarkably, in zz polarization we observe solely the 1281 cm^{-1} mode. This is quite unusual when taking into account that the intensity of the 639 cm^{-1} mode is much weaker than that of the 494 cm^{-1} mode. This symmetry dependence reproduces partially the result reported in Ref. 1 and can hardly be understood within a conventional multiphonon picture. Figures 6(b) and 6(c) display the temperature dependence for x=0.09 and 0.125. The x=0.09 shows a moderate decrease of the second-order maxima upon heating from 5 K to room temperature. In contrast, the FMI sample (x=0.125) exhibits a rather strong suppression of the second-order signal through the metal-insulator transition at $T_C \approx 185$ K, where the rearrangement of orbital ordering takes place.[10] This suggests a relationship between the observed multiphonon scattering and the change of an orbital ordering form through the CAF/FMI phase boundary (see below).

IV. DISCUSSION

In the following, we will examine the origin of the anomalous multiphonon scattering.

Usually, anharmonic electron-phonon interactions can lead to multiphonon scattering in transition metal oxides. The simultaneous emission of n phonons occurs due to lattice anharmonicity. Since this mechanism is a simple extension of a first-order process to higher order, the intensity of

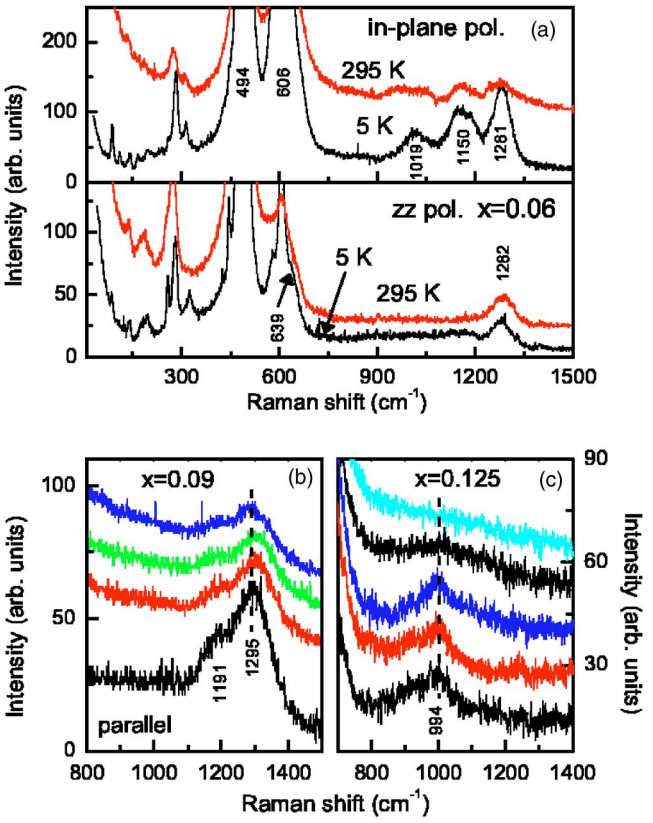

FIG. 6. (Color online) (a) Raman spectra of $La_{0.94}Sr_{0.06}MnO_3$ with in-plane (upper panel) and zz (lower panel) polarization at 5 K and room temperature. (b) and (c) Temperature dependence of second-order Raman spectra of $La_{1-x}Sr_xMnO_3$; for x=0.09 at 295, 200, 100, and 5 K and for x=0.125 at 295, 200, 185, 100, and 5 K, respectively (from upper to lower curve).

n-phonon scattering decays as g^{2n}, where g is the electron-phonon coupling constant. In addition, the intensity ratio of a second- to first-order scattering, that is, I_2/I_1, would be independent of temperature since the respective intensity has the same resonant dependence on incident photon energy.[17] Obviously, these considerations cannot account for (i) the larger intensity of the second-order peak at 1281 cm^{-1} compared to that of the first-order peak at 641 cm^{-1} ($I_2/I_1 \sim 20$ at 5 K), (ii) the anomalous evolution of peak energies in higher-order scattering (see Table I and Fig. 2), and (iii) the temperature-dependent ratio I_2/I_1 [see Fig. 4(b)].

Another effective mechanism is based on resonance scattering. In this process, multiphonons are created by a first-order electron-lattice interaction together with a virtual electron excitation.[17] When the incident photon energy is in resonance with localized electronic excitations, multiphonon scattering becomes enhanced. Very recently, resonant Raman scattering measurements of $LaMnO_3$ reveal a sharp resonance around 2 eV via the creation of *orbiton excitons*.[9] Since in our experiment the incident light energy of 2.34 eV lies in the window of resonance (0.65 eV), the observed multiphonon scattering is also governed by resonant scattering caused by orbitons. Significantly, orbital excitations in the JT ordered state involve a local oxygen displacement.[5] As a consequence, the FC mechanism is expected to be active.

Actually, the validity of the FC mechanism has been corroborated by previous studies.[9,14] Here we point out that the FC mechanism is consistent with the simultaneous observation of similar multiphonon features by optical conductivity and Raman scattering measurements despite completely different selection rules.[2] Infrared inactive modes become infrared active in the multiphonon scattering due to nonlinear local oxygen displacements. In this case, the weak intensity of the multiphonon modes seen in the optical conductivity can be ascribed to orbiton-assisted parity breaking. However, as pointed out above, there exist several anomalies that cannot be captured within the canonical FC picture.

First, the huge ratio of $I_2/I_1 \sim 20$ seen with respect to the Mn–O stretching mode at 641 cm^{-1} is beyond simple theoretical calculations.[5,18] Second, a temperature-dependent ratio I_2/I_1 is expected for the resonant mechanism rather than for the FC one.[19] Third, the observed frequency and intensity of *n*-order scattering (see Fig. 2) is incompatible with the simple FC scenario. We suggest that a strong coupling of orbitons to phonons should also be taken into account.

Self-trapped orbital excitons accompany local ionic distortions; that is, a strong nonlinearity corresponding to a superposition of multiphonons. As a result, orbitons are intrinsically coupled to phonons under electron-phonon coupling. Theoretically, orbiton induced satellites are predicted to develop at higher frequencies of the phonon spectrum.[4] In this scenario, the dominant energy scale of orbiton satellites is determined by the strength of electron-phonon coupling. Noticeably, the anomalous increase of the peak energy is observed at fourth-order scattering between 2096 and 2542 cm^{-1} (see Figs. 1 and 2). If this anomaly is considered to be a result of the influence of orbiton satellites on multiphonon scattering, one can obtain strong electron-phonon coupling of $g \sim 1$.[4] However, orbiton satellites do not show up as separate peaks. Rather, an orbiton-phonon mixed character is reflected in diverse anomalies of the observed multiphonon modes.

This scenario can well explain the observed giant softening of the two-phonon modes by 40 cm^{-1} as a function of temperature [see Fig. 4(a)]. Upon heating, the JT distortions become weaker as demonstrated by the order-parameter-like fall-off of the intensity of the Mn–O bond stretching mode in Fig. 4(a). The weakening of electron-phonon coupling will lead to a shift of the orbiton excitation energy to lower energies.[4] Further evidence is provided by the temperature-dependent ratio of I_2/I_1. With increasing temperature the local JT oxygen displacement caused by the FC process will fade away. Consequently, the FC contribution to multiphonon scattering gradually decreases while reducing the orbiton-phonon mixed character of multiphonon scattering. A crossover of the FC mechanism to a conventional one then results in the reduced lifetime of the orbital exciton seen in Fig. 4(b).

The drastic change of the two-phonon modes through the CAF/FMI phase boundary also supports our interpretation. The three features of the CAF samples turn into a broadened maximum around 1000 cm^{-1} in the $x=0.125$ sample. The comparison between the Sr- and oxygen-doped samples[16] unveils that the broadened maximum around 1000 cm^{-1} at $x=0.125$ results from a softening of the maxima centered around 1300 cm^{-1} at $x=0.09$. Such a giant shift of the two-phonon mode as a function of doping is quite unusual and cannot be understood without considering the orbital degrees of freedom. In the CAF phase a $d_{3x^2-r^2}/d_{3y^2-r^2}$ type of an orbital ordering is stabilized mainly by the cooperative JT distortions, leading to the JT gap of 2 eV. When the incident light energy is within the window of resonance (0.65 eV), Raman scattering process involves an orbital flip of a $d_{3x^2-r^2}/d_{3y^2-r^2}$ orbital ordered state.[9] In this resonant Raman process, the energy and shape of multiphonon scattering are largely determined by a matrix element of orbiton excitons. Thus, the three-peak feature of the observed two-phonon scattering and their polarization dependence should be attributed to the specific orbital ordering pattern of $LaMnO_3$. In the FMI phase, a new type of orbital state evolves from the $LaMnO_3$-type orbital state upon cooling below $T_C \approx 185$ K while suppressing the JT distortions.[10] Although its exact form is not known, there exists evidence that orbital polarons are an essential part of a new orbital ordered state.[10,13] Most probably, thus, the orbital ordering of the FMI phase will be given as a combination of an orbital polaron and a $d_{3x^2-r^2}/d_{3y^2-r^2}$ orbital. Noticeably, the binding energy of orbital polarons, $\Delta_{op}=0.6$ eV, is much smaller than the JT gap of 2 eV.[20] As a result, Raman scattering process will be governed mainly by an off-resonance one, leading to a smearing of the features relying on orbitons. Actually, the three-peak feature changes into the unstructured maximum. In particular, this is related to a fluctuation of the underlying orbitals in the FMI phase.[10,13] The weakening of orbiton-phonon coupling can naturally account for a giant softening of the two-phonon frequency. Therefore, we come to the conclusion that the multiphonon scattering in $LaMnO_3$ relies strongly on the orbital ordered pattern. Furthermore, the intrinsic orbiton-phonon couplings are responsible for the observed anomalous behaviors in intensity and frequency.

V. SUMMARY

In summary, we have reported a detailed study of the higher-order Raman scattering in the manganites $La_{1-x}Sr_xMnO_3$ as a function of temperature and doping. We were able to probe and analyze phonon scattering up to fourth order using Raman spectroscopy. Doping dependence of two-phonon scattering together with the frequency shift of several higher-order modes indicates several anomalies that cannot be understood within the canonical FC mechanism. A full understanding of the multiphonon scattering in the orbital-ordered $LaMnO_3$ system can be achieved by considering the orbito-phonon mixed character. Our study suggests that in orbital ordered systems, multiphonon scattering can serve as a valuable probe of the orbital dynamics.

ACKNOWLEDGMENTS

We thank J. Geck, R. Klingeler, C. Baumann, and M. Grüninger for useful discussions. This work was supported in part by the NATO Collaborative Linkage Grant No. PST.CLG.977766 and INTAS 01-278 as well as by DFG SPP1073.

[1] E. Saitoh, S. Okamoto, K. Takahashi, K. Tobe, K. Yamamoto, T. Kimura, S. Maekawa, and Y. Tokura, Nature (London) **410**, 180 (2001).

[2] M. Grüninger, R. Rückamp, M. Windt, P. Reutler, C. Zobel, T. Lorenz, A. Freimuth, and A. Revcolevschi, Nature (London) **418**, 39 (2002).

[3] E. Saitoh, S. Okamoto, K. Tobe, K. Yamamoto, T. Kimura, S. Ishihara, S. Maekawa, and Y. Tokura, Nature (London) **418**, 40 (2002).

[4] J. van den Brink, Phys. Rev. Lett. **87**, 217202 (2001).

[5] P. B. Allen and V. Perebeinos, Phys. Rev. Lett. **83**, 4828 (1999); V. Perebeinos and P. B. Allen, Phys. Rev. B **64**, 085118 (2001).

[6] Y. Murakami, J. P. Hill, D. Gibbs, M. Blume, I. Koyama, M. Tanaka, H. Kawata, T. Arima, Y. Tokura, K. Hirota, and Y. Endoh, Phys. Rev. Lett. **81**, 582 (1998).

[7] S. Okamoto, S. Ishihara, and S. Maekawa, Phys. Rev. B **65**, 144403 (2002).

[8] S. Okamoto, S. Ishihara, and S. Maekawa, Phys. Rev. B **66**, 014435 (2002).

[9] R. Krüger, B. Schulz, S. Naler, R. Rauer, D. Budelmann, J. Bäckström, K. H. Kim, S.-W. Cheong, V. Perebeinos, and M. Rübhausen, Phys. Rev. Lett. **92**, 097203 (2004).

[10] J. Geck, P. Wochner, D. Bruns, B. Büchner, U. Gebhardt, S. Kiele, P. Reutler, and A. Revcolevschi, Phys. Rev. B **69**, 104413 (2004).

[11] W. Reichardt and M. Braden, Physica B **263–264**, 416 (1999).

[12] M. N. Iliev, M. V. Abrashev, H.-G. Lee, V. N. Popov, Y. Y. Sun, C. Thomsen, R. L. Meng, and C. W. Chu, Phys. Rev. B **57**, 2872 (1998).

[13] K. Y. Choi, P. Lemmens, G. Güntherodt, Yu. G. Pashkevich, V. P. Gnezdilov, P. Reutler, L. Pinsard-Gaudart, B. Büchner, and A. Revcolevschi, Phys. Rev. B **71**, 174402 (2005).

[14] L. Martin-Carron and A. de Andres, Phys. Rev. Lett. **92**, 175501 (2004).

[15] One of the best assignments can be given by the combination of the two peaks, A=493 cm^{-1} and B=641 cm^{-1}: 2A=986, A+B=1134, 2B=1282, 3A=1479, 2A+B=1627, A+2B=1775, 3B=1923, 3A+B=2120, 2A+2B=2268, A+3B=2416, and 4B=2564 cm^{-1} correspond to 985, 1137, 1281, 1485, 1653, 1781, 1911, 2096, 2297, 2418, and 2542 cm^{-1}, respectively. However, this assignment is artificial since multiphonon scattering corresponding to the strongest mode 602 cm^{-1} never appears. Here note that resonant Raman scattering measurements (see Ref. 9) show a simultaneous resonance of the 493 and 602 cm^{-1} modes at the Jahn-Teller gap of 2 eV. Thus, in the incident energy of 2.34 eV two-phonon scatterings should be dominated by an overtone and combination of the above two modes.

[16] Yu. G. Pashkevich, V. P. Gnezdilov, P. Lemmens, K.-Y. Choi, G. Güntherodt, A. V. Eremenko, S. N. Barilo, S. V. Shiryaev, and A. G. Soldatov cond-mat/0506258 (unpublished).

[17] E. Ya. Sherman, O. V. Misochko, and P. Lemmens, *Spectroscopical Studies of High Temperature Superconductors*, edited by N. M. Plakida (Taylor & Francis, London and New York, 2003).

[18] Most probably, the 641 cm^{-1} mode is infrared active (see Ref. 2). Its observation by Raman spectroscopy might be possible through defects/orbitons.

[19] A. E. Pantoja, H. J. Trodahl, A. Fainstein, R. G. Pregliasco, R. G. Buckley, B. Balakrishnan, M. R. Lees, and D. McK. Paul, Phys. Rev. B **63**, 132406 (2001).

[20] R. Kilian and G. Khaliullin, Phys. Rev. B **60**, 13458 (1999).